J. Fluid Mech. (1969), *vol.* 38, *part* 4, *pp.* 689–711
Printed in Great Britain

Breakup of a laminar capillary jet of a viscoelastic fluid

By MICHAEL GOLDIN, JOSEPH YERUSHALMI, ROBERT PFEFFER AND REUEL SHINNAR
The City College of the City University of New York, New York 10031, U.S.A.

(Received 6 October 1967 and in revised form 17 September 1968)

The stability of non-Newtonian jets was investigated. A linearized stability analysis shows that a liquid column of a viscoelastic fluid exhibits more rapid growth of axisymmetric wave disturbances than a Newtonian fluid of the same zero shear viscosity. This result is independent of the form of constitutive equation chosen. Experiments in weakly elastic fluids confirm this expectation, whereas data on fluids with more pronounced elastic properties indicate that non-linear phenomena are dominating. The disturbances appear as a series of droplets connected by random lengths of threads, which thin with distance and eventually lead to jet breakup. Even in dilute viscoelastic solutions, jet breakup does not occur by the growth of clearly defined waves.

1. Introduction

A considerable literature is available on the behaviour of capillary jets of Newtonian fluids; however, very little is known about the behaviour of non-Newtonian fluids. The behaviour of non-Newtonian jets is both of practical and theoretical interest. It is often necessary to design atomization equipment for fluids which are highly non-Newtonian, and yet very little knowledge is available as to what to expect above the general notion that highly elastic fluids are difficult to atomize. From a theoretical point of view this problem is also of interest since a linear stability analysis of Newtonian jets is very successful in predicting the behaviour of these jets under certain conditions (laminar flow). It is therefore tempting to determine whether a linear stability analysis would lead to similar results for viscoelastic fluids.

Middleman (1965), in a recent paper, presents a stability analysis for a capillary jet based on a 3-constant linearized Oldroyd fluid together with some approximate solutions which predict a lower stability for such a fluid as compared to a Newtonian fluid. This is surprising, since experimental evidence involving spinning polymer solutions and melts, as well as experience with Napalm solutions in flame throwers seem to indicate the opposite effect. It is, therefore, of interest to investigate if Middleman's results are only limited to the specific viscoelastic model chosen, or whether they do, indeed, represent the typical behaviour of any viscoelastic material. The present paper, therefore, extends the analysis to a general viscoelastic material. The theoretical results are supple-

mented by experimental studies of the breakup of a cylindrical jet of Newtonian, viscoinelastic and viscoelastic fluids.

2. Theoretical analysis

2.1. *Background*

The capillary instability of a Newtonian jet has been the subject of numerous experimental and theoretical investigations. Most of the analytical solutions stem from the pioneering works of Rayleigh, Weber and Tomotika. Rayleigh (1879) considered the capillary stability of a cylinder of an inviscid fluid; he also discussed the case of a viscous jet without inertia (1882). Weber (1931) obtained the complete linear solution for a viscous jet under surface tension forces in which he also included the action of an inviscid atmosphere. Tomotika (1935) extended the solution to include the effect of a viscous surrounding.

The corresponding analysis for a jet of a viscoelastic fluid may, in practice, be limited by the choice of a specific constitutive equation. However, in the present linear analysis, which rests upon the basic assumption that the jet is initially completely relaxed and is subsequently subjected to very small disturbances, the stability question is found to be dependent only on the properties of a complex viscosity which, in the region of linear behaviour, are clearly defined.

Biot (1945) and Bland (1960, chapter 2) have shown that the rheological properties of any incompressible isotropic viscoelastic material in the region of very small deformations can be described by the following constitutive equation:

$$\tau_{ij} = E\epsilon_{ij} + \eta_\infty \epsilon^*_{ij} + \sum_{r=1}^{N} \int_{-\infty}^{t} C_r e^{-\mu_r(t-\tau)} \epsilon^*_{ij}(\tau)\, d\tau, \tag{1}$$

where τ_{ij}, ϵ_{ij} and ϵ^*_{ij} are the components of the deviatoric stress, linear strain and rate of strain tensors respectively and E, η_∞, C_r and μ_r are all real and positive. The coefficients E (elastic modulus) and η_∞ ($\lim_{\alpha\to\infty} \hat{\eta}(\alpha)$) account for the instantaneous elasticity and the long-term viscous flow respectively. The summation represents a discrete spectrum of relaxation times $1/\mu_r$. Corresponding to equation (1) is a complex viscosity $\hat{\eta}(\alpha)$ obtained *via* a two-sided Laplace transform and defined as

$$\hat{\eta}(\alpha) = \frac{\hat{\tau}_{ij}(\alpha)}{\hat{\epsilon}^*_{ij}} = \frac{E}{\alpha} + \eta_\infty + \sum_{r=1}^{\infty} \frac{C_r}{\mu_r + \alpha}. \tag{2}$$

The complex viscosity $\hat{\eta}(\alpha)$ serves as a compact description of the constitutive equation. It is, in fact, simply the stress–strain rate transfer function for the material and the behaviour of the material can be described in terms of the analytic character of $\hat{\eta}(\alpha)$ considered as a function of the complex variable α.

The rheological properties of viscoelastic materials in the linear region are often expressed in operational form

$$P\tau_{ij} = Q\epsilon_{ij}, \tag{3}$$

where P and Q are polynomials with constant coefficients in the operator $\partial/\partial t$. The complex viscosity corresponding to (3) is given by

$$\hat{\eta}(\alpha) = \frac{\hat{Q}(\alpha)}{\alpha \hat{P}(\alpha)}. \tag{4}$$

This complex viscosity should possess analytic properties which are equivalent to, or suitably approximate, the behaviour of $\hat{\eta}(\alpha)$ of (2). By using the theory of partial fractions Bland (1960) has shown that (4) is identical to (2) if the zeros of $\hat{P}$ and $\hat{Q}$ are all real and non-positive and they alternate, the smallest zero in absolute magnitude belonging to $\hat{Q}$. The polynomial $\hat{Q}$ must also be of a degree one higher than that of $\hat{P}$. Thus, (4) can be properly written as

$$\hat{\eta}(\alpha) = \left[\eta_\infty \prod_{j=1}^{N+1} (\alpha+\lambda_j)\right] \Big/ \alpha\left[\prod_{r=1}^{N} (\alpha+\mu_r)\right], \tag{5}$$

where the $-\lambda_j$ are the zeros of $\hat{Q}$, and correspond to a discrete spectrum of retardation times $1/\lambda_j$. Note that if, for any real material, E or η_∞ or both are zero, equation (2), and subsequently, equation (4) can be readily modified accordingly.

The mathematical analysis of the stability of a linear viscoelastic jet closely parallels Weber's analysis for a Newtonian jet. The results of the present analysis, in fact, include the Newtonian jet as well as the purely elastic jet as special cases.

2.2. *Axisymmetric disturbances*

Consider a cylindrical jet issuing from a circular nozzle into air. The following assumptions are made: (i) the jet is initially relaxed, moving horizontally with a constant velocity, V; (ii) the capillary waves are symmetrical about the jet axis; that is, the jet at all times is circular in cross-section and either expands or contracts; (iii) the fluid is incompressible; (iv) there is no interaction with the ambient air.

Because of the symmetry of the problem, a cylindrical co-ordinate system (r, θ, z) is chosen which moves with a constant velocity V. The linearized equations of motion and continuity are

$$\left.\begin{aligned} \rho\frac{\partial V_r}{\partial t} &= -\frac{\partial p}{\partial r} + \frac{1}{r}\frac{\partial}{\partial r}[r\tau_{rr}] - \frac{\tau_{\theta\theta}}{r} + \frac{\partial \tau_{rz}}{\partial z}, \\ \rho\frac{\partial V_z}{\partial t} &= -\frac{\partial p}{\partial z} + \frac{1}{r}\frac{\partial}{\partial r}[r\tau_{rz}] + \frac{\partial}{\partial z}[\tau_{zz}], \end{aligned}\right\} \tag{6}$$

$$\frac{1}{r}\frac{\partial}{\partial r}(rV_r) + \frac{\partial V_z}{\partial z} = 0, \tag{7}$$

where ρ is the density, V_r and V_z are the velocity components and p is the hydrostatic pressure. The equation for the jet surface disturbed by some wave is

$$r(z,t) = a + \xi(z,t), \tag{8}$$

where a is the unperturbed radius of the jet and $\xi(z,t)$ is the radial displacement of a point on the surface. The boundary conditions specify that the shear stress vanishes on the surface of the jet, and that the radial component of the stress is balanced by the stress induced by the surface tension force. Assuming that ξ is very small compared to a the boundary conditions are expressed as:

$$\left.\begin{aligned} [\tau_{rz}]_{r\approx a} &= 0, \\ [-p+\tau_{rr}]_{r\approx a} &= \frac{\sigma}{a^2}\left[\xi + a^2\frac{\partial^2\xi}{\partial z^2}\right], \end{aligned}\right\} \tag{9}$$

where σ is the coefficient of surface tension. In addition the velocity components along the axis of the jet (at $r = 0$) must be finite.

Application of a two-sided Laplace transform to (6) and (7) results in

$$\left.\begin{aligned}\rho\alpha\hat{V}_r &= -\frac{\partial\hat{p}}{\partial r}+\hat{\eta}(\alpha)\left[\frac{\partial}{\partial r}\left(\frac{1}{r}\frac{\partial}{\partial r}(r\hat{V}_r)\right)+\frac{\partial^2\hat{V}_r}{\partial z^2}\right]\\ \rho\alpha\hat{V}_z &= -\frac{\partial\hat{p}}{\partial z}+\hat{\eta}(\alpha)\left[\frac{1}{r}\frac{\partial}{\partial r}\left(r\frac{\partial\hat{V}_z}{\partial r}\right)+\frac{\partial^2\hat{V}_z}{\partial z^2}\right]\end{aligned}\right\} \tag{10}$$

$$\frac{1}{r}\frac{\partial}{\partial r}(r\hat{V}_r)+\frac{\partial\hat{V}_z}{\partial z}=0, \tag{11}$$

where $\hat{\eta}(\alpha)$ is given by (2). The boundary conditions are similarly transformed. Henceforth the analysis is exactly identical to the corresponding analysis for a Newtonian jet with the constant Newtonian viscosity, η_0, replaced by $\hat{\eta}(\alpha)$. The continuity equation is satisfied by a stream function, ψ, which is related to the velocity components by

$$\hat{V}_r=\frac{1}{r}\frac{\partial\hat{\psi}}{\partial z},\quad \hat{V}_z=-\frac{1}{r}\frac{\partial\hat{\psi}}{\partial r}. \tag{12}$$

Eliminating the pressure from the two equations of motion and introducing the stream function yields

$$\alpha\Delta\hat{\psi}=\hat{\eta}(\alpha)\Delta\Delta\hat{\psi}, \tag{13}$$

where

$$\Delta\equiv\frac{\partial^2}{\partial r^2}-\frac{1}{r}\frac{\partial}{\partial r}+\frac{\partial^2}{\partial z^2}.$$

The solution to this equation with assumed periodicity in the axial z direction is

$$\hat{\psi}=r[C_1I_1(kr)+C_2I_1(lr)+C_3K_1(kr)+C_4K_1(lr)]e^{-ikz}, \tag{14}$$

where

$$l^2=k^2+\frac{\rho\alpha}{\hat{\eta}(\alpha)}.$$

The quantity k is the wave-number of a disturbance wave and is related to the wavelength, δ, by $\delta = 2\pi/k$, I_n and K_n are modified Bessel functions of order n, and C_1, C_2, C_3, C_4 are arbitrary constants. Application of the boundary conditions leads to the secular or characteristic equation which relates α and k:

$$\alpha^2+\frac{2\hat{\eta}(\alpha)k^2}{\rho I_0(ka)}\left[I_1'(ka)-\frac{2kl}{k^2+l^2}\frac{I_1(ka)}{I_1(la)}I_1'(la)\right]\alpha=\frac{\sigma k}{2\rho a^2}[1-k^2a^2]\frac{I_1(ka)}{I_0(ka)}\frac{l^2-k^2}{l^2+k^2}, \tag{15}$$

where $I_n'(\ )$ denotes differentiation of the Bessel function with respect to the argument. Equation (15) is in general very complex and cannot be solved analytically. However, for small arguments, the Bessel functions can be approximated by the leading terms of their expansions. The resulting equation is

$$\alpha^2+\frac{3k^2}{\rho}\hat{\eta}(\alpha)\alpha-\frac{\sigma k^2}{2\rho a}(1-k^2a^2)=0. \tag{16}$$

The above approximation corresponds to conditions of practical interest where the wavelengths of the disturbances are much greater than the radius of the unperturbed jet.

Solution of the characteristic equation yields the rate of growth of unstable wave-like disturbances; these correspond to the positive real parts of the characteristic values of α. For infinitesimal disturbances of the same initial magnitude, droplet formation will be controlled by the particular wave which grows most rapidly.

The fastest growing wave can be found by implicit differentiation of (16), and letting $d\alpha/dk = 0$ (the existence of a real positive α is shown in the subsequent discussion). The fastest growing rate, α^*, can, in this way, be obtained from the following expression

$$\alpha^*\left[2+3\frac{\hat{\eta}(\alpha^*)}{\rho}\sqrt{\left(\frac{2\rho}{\sigma a}\right)}\right]=\sqrt{\left(\frac{\sigma}{2\rho a^3}\right)}. \tag{17}$$

The corresponding wave-number is obtained from

$$k^{*2}=\alpha^*\sqrt{\left(\frac{2\rho}{\sigma a}\right)}. \tag{18}$$

For a Newtonian fluid, $\hat{\eta}(\alpha)=\eta_0$, and equations (17) and (18) yield

$$\alpha_0^*=\sqrt{\left(\frac{\sigma}{2\rho a^3}\right)}\Big/\left(2+\frac{3\eta_0}{\rho}\sqrt{\left(\frac{2\rho}{\sigma a}\right)}\right), \tag{19}$$

$$k_0^*=\left[3\eta_0 a\sqrt{\left(\frac{2a}{\rho\sigma}\right)}+2a^2\right]^{-\frac{1}{2}}. \tag{20}$$

The zero subscript in α_0^* and k_0^* denotes Newtonian values. The dimensionless wavelength is obtained as

$$\frac{\delta_0}{2a}=\pi\sqrt{2}\left[1+\frac{3\eta_0}{\sqrt{(2a\rho\sigma)}}\right]^{\frac{1}{2}}. \tag{21}$$

An experimental measure of the stability of a jet is the length of the coherent portion of the jet, defined as the breakup length, L, which is given by

$$L=CV/\alpha^*, \tag{22}$$

where C is a constant which depends on the initial magnitude of the disturbance, and must be determined experimentally. Equations (19) and (22) can be combined to give the dimensionless breakup length as

$$\frac{L}{2a}=C\left[We^{\frac{1}{2}}+3\frac{We}{Re}\right], \tag{23}$$

where $We=2\rho aV^2/\sigma$ is the Weber number and $Re=2\rho Va/\eta_0$ is the Reynolds number.

No simple expression for α^* can be obtained for a viscoelastic jet in view of the relative complexity of $\hat{\eta}(\alpha)$. The value of α^* can, however, be readily computed numerically when $\hat{\eta}(\alpha)$ assumes a simple form.

It is of great interest to compare the stability of a viscoelastic jet with respect to a jet of Newtonian fluid. For this purpose (17) is divided through by

$$\left[2+\left(\frac{3\eta_0}{\rho}\right)\sqrt{\left(\frac{2\rho}{\sigma a}\right)}\right];$$

using (19) one obtains

$$\frac{[2+(3/\rho)\hat{\eta}(\alpha^*)\sqrt{(2\rho/\sigma a)}]}{[2+(3/\rho)\eta_0\sqrt{(2\rho/\sigma a)}]} = \frac{\alpha_0^*}{\alpha^*}. \tag{24}$$

From (24) it is clear that the value of the ratio α_0^*/α^* depends on the relative magnitude of $\hat{\eta}(\alpha)$ with respect to η_0. Recalling the expression for $\hat{\eta}(\alpha)$

$$\hat{\eta}(\alpha) = \frac{E}{\alpha} + \eta_\infty + \sum_{r=1}^{N} \frac{C_r}{\mu_r + \alpha}, \tag{2}$$

we can distinguish between two classes of behaviour:

(*a*) When $E = 0$ in (2), the material behaves as a real fluid in the sense that, for very slow deformations ($\alpha \to 0$), the material behaves as a Newtonian fluid of viscosity $\eta_0 = \hat{\eta}(0)$, with $\hat{\eta}(0)$ given by

$$\hat{\eta}(0) = \eta_\infty + \sum_{r=1}^{N} C_r/\mu_r. \tag{25}$$

In this case $\hat{\eta}(\alpha)$ is a monotonically decreasing function of α with η_∞ as the lower bound. Consequently $\hat{\eta}(\alpha^*) < \hat{\eta}(0)$ and according to (24) such a jet is less stable than a Newtonian jet of viscosity $\eta_0 = \hat{\eta}(0)$. The same conclusion can also be deduced from a simple geometrical argument which also confirms the existence of a real positive α^*. For a fixed value of k, (16) can be written as

$$\hat{\eta}(\alpha) = \frac{B}{\alpha} - B'\alpha, \tag{26}$$

where

$$B = \frac{\sigma(1-k^2a^2)}{6a}; \quad B' = \frac{\rho}{3k^2}.$$

For a Newtonian fluid $\hat{\eta}(\alpha) = \eta_0$; therefore, referring to figure 1 (in which both sides of (26) are plotted as a function of α) it is clear that as long as B is positive ($ka < 1$), a positive real root of α will always exist (point 1 in figure 1). In the case of a viscoelastic fluid with $\hat{\eta}(\alpha)$ bounded by η_0 and η_∞, figure 1 again shows the existence of a positive real α (point 2 in figure 1). Furthermore, it can be generally concluded that for any value of k for which a Newtonian fluid of viscosity η_0 is unstable (with α real and positive) a viscoelastic fluid with $\hat{\eta}(0) = \eta_0$ has a real positive α which is larger in magnitude than the corresponding α of the Newtonian fluid. If we construct a plot of α *vs.* k^2 (see figure 2), the curve for any viscoelastic fluid with finite $\hat{\eta}(\alpha)$ will lie above the curve corresponding to a Newtonian fluid of the same zero viscosity and below the curve corresponding to an inviscid fluid with all curves crossing the k axis at the same points. In this sense a jet of such a fluid is less stable than a Newtonian jet relative to small disturbances. Any experimentally observed higher stability must, therefore, be due to non-linear phenomena or, alternatively, the fluid may not be a true fluid in the sense that it is characterized by a complex viscosity with $E \neq 0$. This brings us to the second class of behaviour.

(*b*) When E is finite in (2) and all the μ_r are zero, we deal with a material which displays a purely elastic behaviour and for which

$$\hat{\eta}(\alpha) = E/\alpha. \tag{27}$$

Referring again to (26) and to figure 3 it is seen that if $E < B$ there will always be a positive real α (point 1 in figure 3). When $E > B$, however, no positive root exists and the jet is unconditionally stable. If $\mu_r \neq 0$ we find similarly that when $E > B$ the jet is unconditionally stable whereas for any viscoelastic material with $E < B$ there exists a real positive α causing instability. However, in this

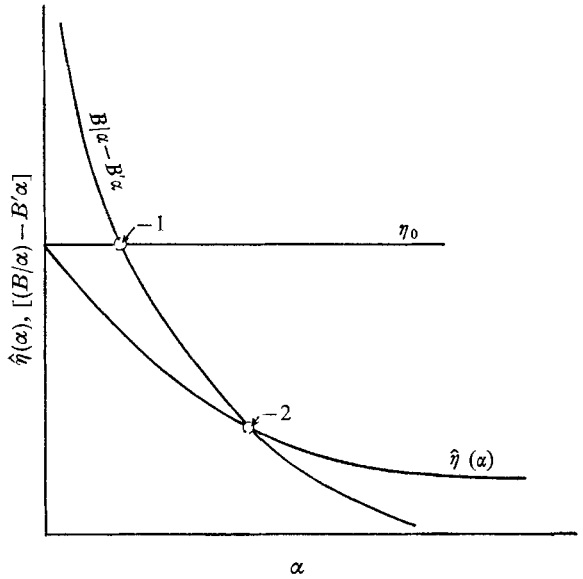

FIGURE 1. Qualitative representation of equation (26) for a Newtonian fluid of viscosity η_0 and a viscoelastic fluid with $\hat{\eta}(0) = \eta_0$.

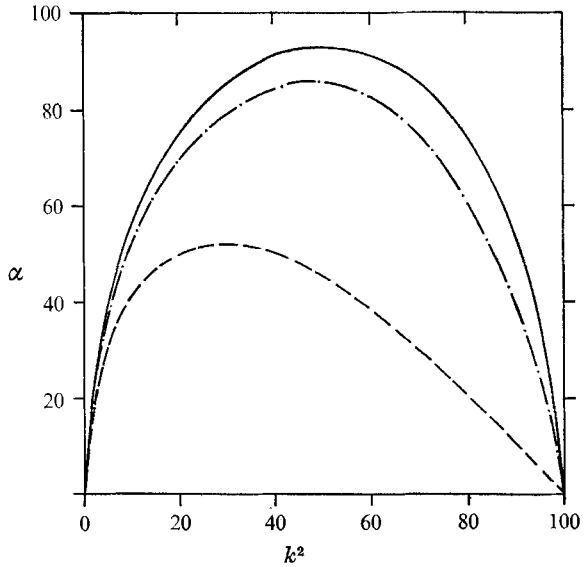

FIGURE 2. A plot of α *vs.* k^2 for three fluids. ———, inviscid fluid $\hat{\eta}(\alpha) = 0$; — — —, Newtonian fluid $\eta_0 = 1$; —·—·—, viscoelastic fluid with $\hat{\eta}(\alpha) = \eta_0/(1+\lambda\alpha)$, $\eta_0 = 1$, $\lambda = 0{\cdot}1$, $\sigma = 70$, $\rho = 1$, $a = 0{\cdot}1$. All values are in CGS units.

case it is meaningless to talk about the effect of viscoelasticity on the stability of the jet since there is no obvious basis for comparison.

Most of the recent theoretical works on non-Newtonian flow deal with fluids for which $\hat{\eta}(0)$ is finite. Real viscoelastic fluids, however, might have some

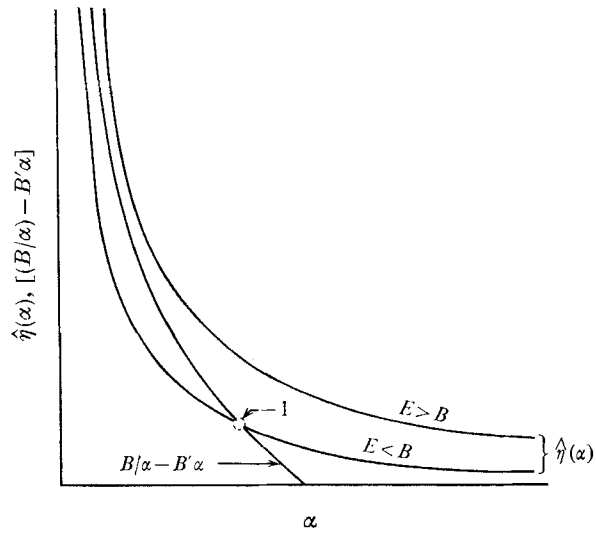

FIGURE 3. Qualitative representation of equation (26) for a purely elastic body of modulus E.

inherent structure and therefore, a yield value. Such fluids could lead to completely stable jets based on the arguments given above.

2.3. *Asymmetric disturbances*

The stability of a viscoelastic jet with respect to asymmetric disturbances can be analyzed by a method similar to the one used above. However, by considering deformations whose wavelengths are large compared to the unperturbed radius of the jet, the appropriate characteristic equation can be obtained directly from the equations of motion by recognizing that, under these circumstances, V_z can be considered independent of the radial direction r, and furthermore, that $V_z \gg V_r$. With these assumptions the dynamic equation becomes

$$\rho\alpha\hat{V}_z = 3\hat{\eta}(\alpha)\frac{\partial^2\hat{V}_z}{\partial z^2} + \frac{\partial\hat{p}_\sigma}{\partial z}, \tag{28}$$

where

$$\hat{p}_\sigma = \frac{\sigma}{a^2}\left[\hat{\xi} + a^2\frac{\partial^2\hat{\xi}}{\partial z^2} + \frac{\partial^2\hat{\xi}}{\partial\theta^2}\right],$$

p_σ is the stress due to surface tension traction and $\xi(z,t)$ is related to V_z *via* the continuity equation

$$\frac{\partial V_z}{\partial z} = -\frac{2}{a}\frac{\partial\xi}{\partial t} \quad \text{or} \quad \frac{\partial\hat{V}_z}{\partial z} = -\frac{2}{a}\alpha\hat{\xi}. \tag{29}$$

Differentiating (28) with respect to z and substituting (29) yields

$$\alpha^2\hat{\xi} - 3\frac{\hat{\eta}(\alpha)}{\rho}\alpha\frac{\partial^2\hat{\xi}}{\partial z} + \frac{\sigma}{2\rho\alpha}\left(\hat{\xi} + \frac{\partial^2\hat{\xi}}{\partial\theta^2} + a^2\frac{\partial^2\hat{\xi}}{\partial z^2}\right) = 0. \tag{30}$$

$\hat{\xi}(\alpha)$ is assumed to be of the form

$$\hat{\xi} = \sum_{s=0}^{\infty} \xi_s^0 e^{ikz}\cos(s\theta + \Omega), \tag{31}$$

where Ω is a suitable phase shift and ξ_s^0 is the initial amplitude of a disturbance wave. Substituting (31) into (30) results in the following characteristic equation

$$\alpha^2 + \frac{3k^2}{\rho}\hat{\eta}(\alpha)\alpha - \frac{\sigma k^2}{2\rho a}[1 - s^2 - k^2a^2] = 0. \tag{32}$$

For axisymmetric waves $s = 0$, and equation (32) is identical to (16) which has been obtained before. Letting $s = 1$ corresponds to a displacement of the jet axis about its original straight line, with the cross-section remaining circular at all times; $s = 2$ corresponds to waves with elliptical cross-sections in which the vertical and the horizontal semiaxes alternate along the axis of the jet. Higher modes correspond to still different configurational deformations.

It follows from (32) that a jet of fluid obeying a linear constitutive equation is completely stable with respect to asymmetric disturbances with wavelengths that are larger than the free radius of the jet.

2.4. *Discussion of theoretical results*

It has been shown that if the jet instability is dominated by a real latent root α^*, and if the complex viscosity is bounded in absolute value by η_0, then the jet is less stable than a Newtonian jet of viscosity η_0. On the other hand when $\hat{\eta}(\alpha)$ is unbounded the jet may become completely stable, and no meaningful basis of comparison can be established for the behaviours of such a jet and a jet of a Newtonian fluid. The analysis which led to these conclusions is subject to several assumptions whose validity must be assessed before the results can be evaluated in the light of the experimental data.

One of the underlying assumptions in the present analysis is that the jet is completely relaxed initially. In reality, the free jet experiences a stress relaxation in a region near the exit nozzle. Whereas for low-speed Newtonian jets this region is negligibly short in length, the corresponding length for viscoelastic jets may be significant and thus strongly affect the subsequent stability of these jets. The use of a constitutive equation in which $\hat{\eta}(\alpha)$ assumes the form given by (2) is valid only when the initial profile is virtually relaxed; should the stress relaxation occur along a significant portion of the jet, the use of this model ceases to be valid. The validity of the linear theory of viscoelasticity is also questionable for the case in which infinitesimal disturbances are superimposed upon finite deformations. Furthermore, in contrast to a Newtonian fluid, the flow of a viscoelastic fluid inside the capillary tube is accompanied by generation of normal stresses; the decay of these stresses along the free jet cannot be

accounted for by the linear theory. In the final analysis, one has to weigh the validity of the assumption regarding the initial relaxed profile in the light of the experimental conditions and the properties of the fluid of interest.

The next obvious question bears upon the validity of a linear stability analysis. The present analysis presupposes the existence of wave-like disturbances whose initial amplitudes are of infinitesimal order of magnitude as compared to the wavelengths of the disturbances. The stability of the jet is, therefore, analyzed relative to these disturbances. Consequently, one can neglect the non-linear terms in the equations of motion and, at the same time, employ a linear constitutive equation in place of a more general, non-linear, constitutive equation which is capable of describing all viscoelastic phenomena. If in the course of their growth, the amplitudes of the disturbances attain a moderate size, the linear theory can no longer be considered applicable and the subsequent stability of the jet must be investigated with due account to non-linear effects.

In the case of low-speed Newtonian jets, the linear theory leads to results which are in excellent agreement with the experimental data despite the fact that the amplitude of the disturbance wave does attain a moderate size in a relatively short time interval. This may seem to indicate that the non-linear effects inherent in the equations of motion do not alter significantly the growth of disturbances on the surface of a low-speed Newtonian jet. On the other hand, the complete description of a viscoelastic jet involves, in addition to the non-linear inertia terms of the momentum equations, a non-linearity which is inherent in the rheological properties of the fluid. The stability of a viscoelastic jet relative to finite disturbances may, therefore, be governed by non-linear effects. The linear theory attempts to describe the stability of the jet relative to infinitesimal disturbances and in this sense it is completely valid. However, as will be discussed in the next sections, the linear theory fails to explain satisfactorily the observed behaviour of capillary jets of polymer solutions.

3. Experimental studies

The equipment and techniques used in these studies are straightforward and require only brief explanation. Either an Instron mechanical tester or pressurized nitrogen activated the piston of a hydraulic cylinder which contained the test fluid. The liquid flowed from the cylinder, through a section of reinforced rubber hose and past a $50\,\mu$ filter. These served to minimize mechanical vibrations that might be present in the Instron from being transmitted along the walls of the metal piping or through the fluid itself and also to trap any contaminant particles. The fluid then entered a cube designed to house a pressure transducer and the capillary. This unit was mounted on a concrete block to dampen vibrations from the surroundings. Nozzles were fashioned from hypodermic needles by grinding their tips to a flat face. The bores were examined under 100 power magnification for concentricity and surface imperfections. The $L/2a$ ratios ranged from $L/2a = 50$–200.

Still photographs were taken with a 4×5 bellows camera equipped with a Polaroid back while motion pictures were made with a 400 ft. capacity, high-speed

Hycam camera. EG & G single flash and strobe units provided the microsecond duration, high intensity lighting.

The range of experimental variables included jet velocities from 250 to 3000 cm/sec and nozzle diameters between 0·0216 and 0·158 cm.

3.1. *Test fluids*

The test fluids consisted of a number of water soluble polymers (see table 1) dissolved in distilled water under conditions minimizing shear and thermal

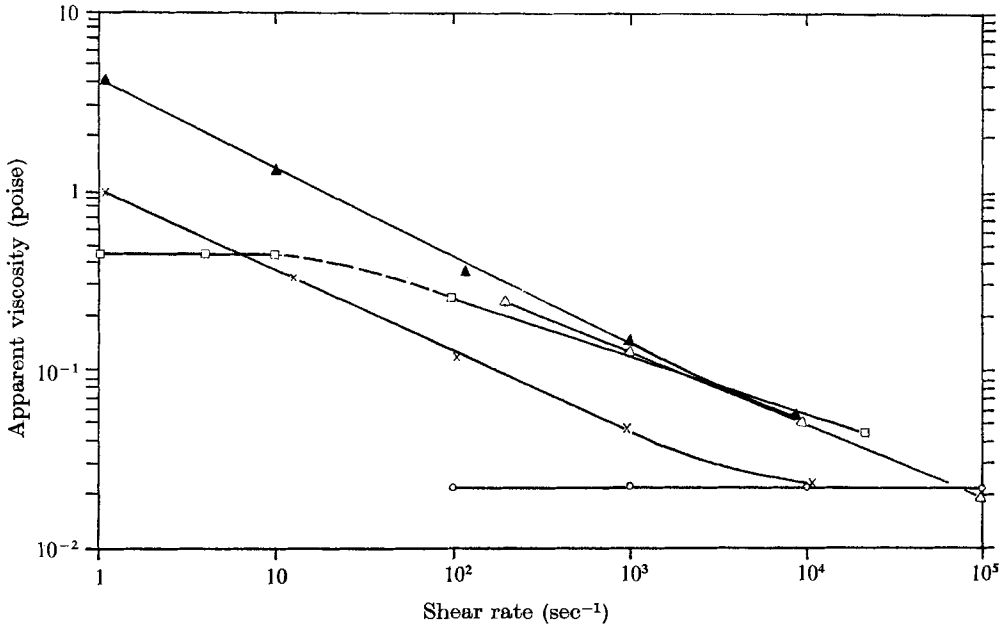

FIGURE 4. Published data of apparent viscosity *vs.* shear rate for the test fluids. ○, 0·5 % Guar Gum (J-2P), Wells (1965); ×, 0·05 % Separan AP 30; ▲, 0·25 % Separan AP-30, Schwarz (1968); △, 0·25 % Separan ET-597, Seyer (1967); □, 0·25 % SCMC 70S, Merrill (1959).

degradation. Values of density and surface tension for the polymeric solutions were of the same order as water. A summary of published viscosity *vs.* shear rate data for some of the test fluids is shown in figure 4. Zero shear viscosities were determined or estimated from our measurements and additional information from Turian (1964), Schwarz (1968), Wells (1965) and Merrill (1959). These are given in table 1.

Huppler (1965) and Hurd (1962) have characterized Carbopol as a non-Newtonian inelastic fluid exhibiting a shear dependent viscosity but possessing very small normal forces. Several investigators, including Dodge & Metzner (1959) and Kapoor (1963), have demonstrated that Carbopol solutions are not drag reducing nor do they display any recoil phenomena. All the other polymeric liquids show sharp reduction in drag over that expected for Newtonian fluids and are considered to be viscoelastic. Shertzer (1965) has found appreciable

normal forces to exist in Separan solutions. Measurements of normal forces were extended by Oliver (1966) to include Separan, Polyox and SCMC at concentrations down to the 0·01 % level. Using a three constant Oldroyd model on 0·45 %

Polymer	Concentration (%)	Zero shear viscosity
Carbopol 934 (B. F. Goodrich Co.)	0·10	5–10* poise
Separan AP30 (Dow Chemical Co.)	0·05†	0·50
	0·25†	10·0
Sodium Carboxy-Methyl Cellulose Type 7HS (Hercules Powder Co.)	0·25	0·45
Polyox-Coagulant (Union Carbide Corp.)	0·25‡	2–5*
Guar Gum (Stein Hall Corp.)	0·05§	0·022

* Estimated.
† Small amounts of glycerin added for stability.
‡ Small amounts of isopropanol added for stability.
§ Small amounts of formaldehyde added to prevent bacterial growth.

TABLE 1. Polymeric solutions used in experimental investigation.

Separan data at low shear rates, the molecular relaxation time can be estimated to be of the order of 0·25 sec.

3.2. *Qualitative observations*

Marked differences were found to exist between the behaviour of Newtonian, non-Newtonian inelastic and viscoelastic jets. The distinctions are exemplified by the photographs of figure 5, plate 1, which show typical appearances of the jets formed by each class of fluids. In Newtonian jets, examples of which are water and ethylene glycol, an infinitesimal disturbance generated within the capillary is propagated as an exponentially growing wave with a constant wavelength. At low velocities, where the influence of the surroundings may be neglected, the growth rate and wavelength of the disturbance may be accurately predicted from Weber's theory, equations (19) and (21). The breakup length is unambiguous, reproducible and readily measurable from photographs. A non-Newtonian inelastic jet of 0·1 % Carbopol appears to have characteristics similar to those shown by Newtonian fluids, that is; a disturbance is propagated as an exponentially growing wave of constant wavelength.

Solutions of 0·25 % SCMC are elastic and the jets initially show a growing wave with a clearly defined wavelength. The growth of the wave is, however, arrested before breakup and a string of droplets connected by thin threads is formed. The droplets are found at regular distances from each other indicating their formation from a wave of constant wavelength. This behaviour is shown in the sequence of photographs of figure 6, plate 1. Secondary instabilities in the form of very small droplets may also develop on the threads as seen in the last photograph of this figure. In 0·25 % Separan and 0·25 % Polyox, which are considerably more elastic than 0·25 % SCMC, no wave formation is discernible and the first visible disturbance appears as a large droplet, isolated in space from any

systematic growth pattern. The distances between droplets are randomly distributed and are connected by threads which thin with distance, eventually leading to the breakup of the liquid column. A series of photographs taken along the length of a 0·25 % Separan jet illustrates these phenomena and is seen in figure 7, plate 2. The behaviour of a 0·25 % Polyox jet is similar to that shown by 0·25 % Separan. At high velocities the threads are able to undergo large amplitude, three-dimensional disturbances without breaking. This behaviour is shown in photograph (*a*) of figure 9, plate 3. With more concentrated viscoelastic solutions (0·5 % Separan) no observable disturbances were detected within the limits of the 6 ft. jet length which could be conveniently photographed.

Dilute viscoelastic jets such as 0·05 % Separan display an intermediate behaviour in that the disturbance is initially propagated as a wave of uneven amplitude whose wavelength increases with distance. Gradually the waves form a string of droplets connected by threads, as in the 0·25 % Separan and 0·25 % Polyox jets. The droplet distribution, while not completely random, is less regular than in 0·25 % SCMC. The photographs of figure 8, plate 2, show how a 0·05 % Separan jet changes in appearance from an initial wave-like contour to a configuration consisting of droplets connected by threads. The threads are seen to thin with distance from the nozzle, and at the same time, the droplet diameter increases. Jet breakup results from disruption of a thinning thread. In this dilute viscoelastic jet there is a preponderance of 'twin' droplets in juxtaposition and separated from the rest by long threads. Photograph (*d*) of figure 8 illustrates the interesting symmetry of the 'twin' droplets.

Another type of instability in which the liquid column possesses a screw orientation has been observed with dilute viscoelastic jets. There is only a narrow velocity range where this phenomena is distinctly visible. Photographs (*b*) and (*c*) of figure 9 show a 0·05 % Guar Gum jet travelling at a velocity of 350 cm/sec and forming a stable helix whose pitch increases with distance from the nozzle. Near breakup, a disturbance wave with an identifiable wavelength can be seen superimposed upon the helix. Another example of a screw instability can be seen in the photographs (*d*)–(*i*) of figure 9 for a 0·05 % Separan jet moving with a velocity of 690 cm/sec. The disturbance develops close to the nozzle but later dampens out and finally reverts to the droplet thread configuration characteristic of viscoelastic jets. The screw instabilities resemble the shapes observed with molten polymers undergoing melt fracture.

Figures 5–9 have served to qualitatively demonstrate the difference between Newtonian, non-Newtonian inelastic and viscoelastic jets. In the following sections a more detailed and quantitative discussion will be presented.

3.3. *Newtonian and viscoinelastic jets*

The wavelengths of disturbance waves propagating in Newtonian and 0·1 % Carbopol jets were measured over a range of velocities and nozzle diameters. Typical data are given in table 2. As predicted from Weber's theory (equation (21)), the wavelength of a low speed jet is independent of velocity. Good agreement was obtained between the theoretical wavelengths for Newtonian fluids and the experimental values. The disturbance wavelength for a 0·1 % Carbopol

jet corresponds to that of an inviscid liquid, which would be expected at these high shear conditions for a fluid with a shear dependent viscosity, if its molecular relaxation time were of the same order as the jet breakup time.

Liquid or solution	Nozzle diameter (cm)	Jet velocity (cm/sec)	Experimental wavelength	Theoretical wavelength
Water	0·0263	190	0·08–0·10	0·12
		310	0·10	0·12
75 % glycerin–water	0·0868	270	0·49	0·45
0·1 %	0·0414	300	0·15	0·19*
Carbopol		440	0·15	0·19*
0·1 %	0·0868	310	0·35	0·39*
Carbopol		410	0·35	0·39*

* Calculated for an inviscid fluid.

TABLE 2. Comparison of calculated and measured wavelengths for Newtonian and 0·1 % Carbopol jets.

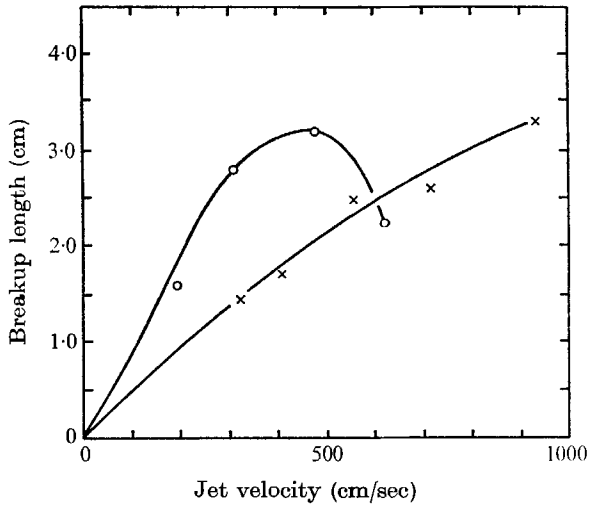

FIGURE 10. Breakup length of water and 0·1 % Carbopol jets as a function of jet velocity. ○, water; ×, 0·1 % Carbopol. Nozzle diameter, 0·0263 cm.

The stability of 0·1 % Carbopol was compared to that of water, which behaves as an inviscid liquid under these conditions, by plotting breakup length *vs.* jet velocity for a 0·0263 cm nozzle. As seen in figure 10, when both curves are linear, the stability of the ideal fluid is greater than that of the non-Newtonian inelastic fluid. This result is surprising since the viscosity of 0·1 % Carbopol is higher than that of water at all shear rates and yet their surface tensions are equivalent. A more dramatic comparison is shown in the photograph of figure 11, plate 3, where the breakup length of water is seen to be $2\frac{1}{2}$ times greater than for 0·1 % Carbopol at the same jet velocity and nozzle diameter. However, as seen from figure 10, the viscous consistency of 0·1 % Carbopol does inhibit breakup due to air resistance. The maximum in its L *vs.* V curve occurs at much higher velocities than that for water.

Weber's analysis for Newtonian jets, equation (23), predicts that $L/2a$ is proportional to $(2a)^{\frac{1}{2}}$ for a low viscosity fluid and is independent of $(2a)$ for a high viscosity liquid. This result was confirmed by the Newtonian jet experiments. Breakup length *vs.* jet velocity data for 0·1 % Carbopol, taken from the linear portion of the complete curve, are plotted in figure 12 and show stability to increase with velocity and nozzle diameter. At constant velocity, $L/2a$ was

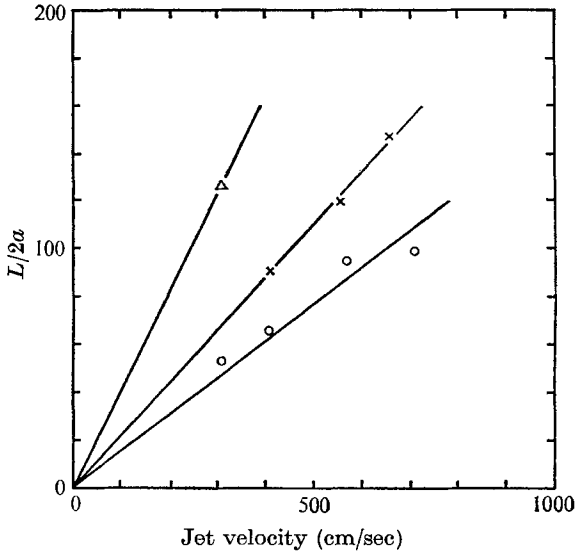

FIGURE 12. Breakup length of 0·1 % Carbopol jet in the laminar flow region as a function of jet velocity and nozzle diameter. Nozzle diameter: ○, 0·0263 cm; ×, 0·0414 cm; △, 0·0868 cm.

found to be proportional to $(2a)^{\frac{1}{2}}$, which indicates that a 0·1 % solution of Carbopol behaves quite similar to an inviscid liquid.

3.4. *Viscoelastic fluids*

Solutions of 0·25 % SCMC form jets which initially propagate disturbances as a growing wave with a constant wavelength. In Newtonian jets, there is almost no difference between the place where the wave amplitude is strongly evident and the place of final breakup. However, as seen in figure 6, the growth of the wave in 0·25 % SCMC jets is arrested and strings of droplets connected by thinning threads are formed. Final breakup occurs much later and in this region of nonlinear disturbances the predictions of linear theory are inapplicable. The breakup length for 0·25 % SCMC jets is therefore defined as the distance from the nozzle where the disturbance wave amplitude is comparable to the original jet radius. Using this criterion, the breakup length and wavelength are found to lie between those predicted for an inviscid jet and those for a Newtonian fluid of the same zero shear viscosity, which is in agreement with the theoretical predictions. Typical data are found in table 3.

Viscoelastic jets of 0·25 % Separan and 0·25 % Polyox in figures 5 and 7 have shown that those fluids possess a unique initial disturbance distance, which

represents the distance from the nozzle to the sudden appearance of a large droplet. Values for this distance are not as reproducible as for Newtonian jet breakup length and were found to vary by $\pm 30\,\%$. The initial disturbance length for a 0·25 % Separan jet, as shown in figure 13, increases with velocity and nozzle diameter. A crossplot of the data, taken at a velocity of 400 cm/sec

Nozzle diameter (cm)	Jet velocity (cm/sec)	Theoretical breakup length (cm) $\hat{\eta}(0)=0$ cp	Theoretical breakup length (cm) $\hat{\eta}(0)=45$ cp	Experimental breakup lengths (cm)	Theoretical wavelength $\hat{\eta}(0)=0$ cp	Theoretical wavelength $\hat{\eta}(0)=45$ cp	Experimental wavelength (cm)
0·0216	309	1·8	3·3	2·5	0·099	0·14	0·12
	426	2·3	4·4	3·3	0·099	0·14	0·11

TABLE 3. Breakup length and wavelength of 0·25% SCMC jets compared to Newtonian jets

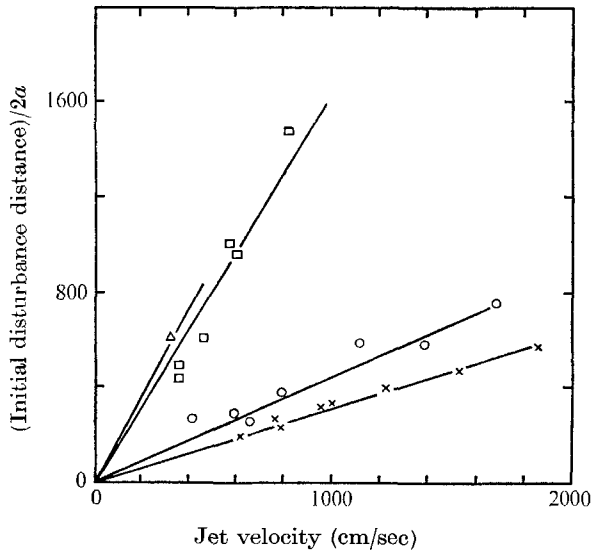

FIGURE 13. Ratio of initial disturbance distance to nozzle diameter for a 0·25 % Separan jet as a function of jet velocity. Nozzle diameter: ×, 0·0216 cm; ○, 0·0263 cm; □, 0·0414 cm; △, 0·0868 cm.

is given in figure 14 and shows the initial disturbance length/nozzle diameter ratio to be a strong function of diameter. As the nozzle diameter increases, the fluid becomes less sheared and the initial disturbance length/nozzle diameter ratio becomes independent of diameter. This result would be expected for a highly shear sensitive liquid.

The breakup length of the dilute (0·05 %) and the more concentrated (0·25 %) Separan jets based on the point where the threads break, is shown in figure 15 as a function of jet velocity. Determination of this distance was made by visual

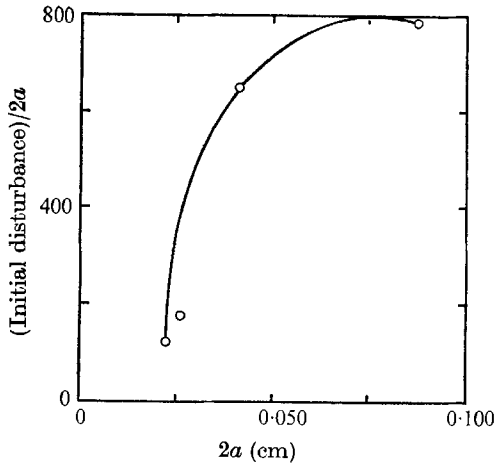

FIGURE 14. Effect of nozzle diameter on initial disturbance length at constant jet velocity for a 0·25 % Separan jet. Jet velocity = 400 cm/sec.

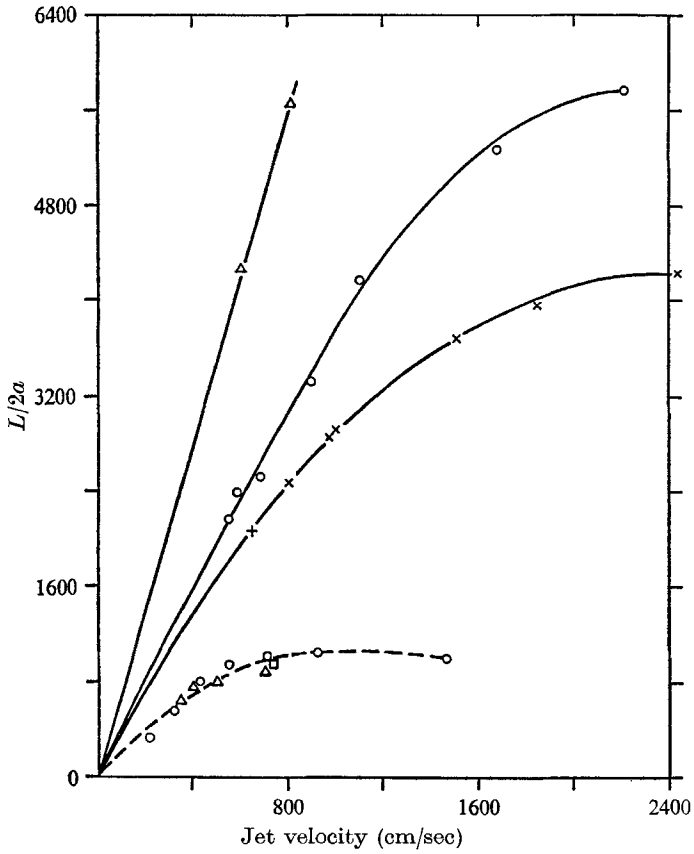

FIGURE 15. Breakup length of 0·05 % Separan and 0·25 % Separan jets as a function of jet velocity and nozzle diameter. Nozzle diameter: ×, 0·0216 cm; ○, 0·0263 cm; △, 0·0414 cm; □, 0·0868 cm; – – –, 0·05 % Separan; ——, 0·25 % Separan.

observation of the liquid column under stroboscopic light and the accuracy of these measurements therefore depends upon the ability to detect the finest threads. Values were found to be reproducible to within $\pm 10\,\%$. The breakup length is seen to be initially linear with velocity and then becomes independent of it. This behaviour is very different from that for a Newtonian or a non-Newtonian inelastic jet. The breakup length for these fluids is also initially linear with jet velocity but, when air resistance becomes significant, the curve goes through a maximum and further increases in jet velocity result in a decrease in breakup length. As the flow within the capillary becomes turbulent the breakup length again increases linearly with jet velocity. A detailed description of these changes for Newtonian jets is presented by Grant & Middleman (1966).

The 'droplet-thread' configuration is the form eventually assumed by both the dilute and the more concentrated viscoelastic jets. Threads are seen to thin with increasing distance from the nozzle while the droplet diameter increases. By photographing a 0·25 % Separan jet along its length until breakup occurred, the droplet diameter and thread length were determined as a function of distance along the liquid column. The droplet size slowly increased to approximately 1·5 times its original diameter until about half-way from the breakup point; thereafter it remained constant. The ratio of the Sauter mean diameter, D_s, and the weight average mean diameter, D_w, were also constant in this region, where the average droplet diameter is still increasing; selected frames are shown in photographs (*a*)–(*f*) of figure 16, plate 4. The droplets do not all move at the same velocity along the threads and, as a result, collisions occur, creating new droplets of larger diameter. Smaller particles decelerate more rapidly than larger particles because of air friction and this would lead to collisions of the type observed. Of course, this does not explain why the viscoelastic jet forms the 'droplet-thread' configuration in the first place. Photographs (*g*)–(*j*) of figure 16 show an instance where a whole section of the jet overtakes another section which was previously several centimetres in front of it and then passes it. This phenomenon is not as yet understood.

The thread lengths between droplets were also analyzed as a function of distance from the nozzle but were found to be widely distributed and showed no discernible pattern. At any one location, the values ranged from fractions of a centimetre to 6 cm with an average of 2·5 cm. Thread lengths of the dilute viscoelastic jet (0·05 %) Separan vary in a similar manner except that the threads are shorter.

While thread thinning data for all viscoelastic jets show considerable scatter, a dimensionless plot of the fraction of original radius a'/a *vs.* the fraction of breakup length, L'/L, has the form shown in figure 17. Here a' represents the jet radius at a distance L' from the nozzle tip. Thus, breakup of the jet by disruption of the thinnest thread is imminent when the thread diameter is approximately $\frac{1}{4}$ of the original diameter. Just before breakup occurs, the threads thin quite rapidly. In this region the stability of the threads is quite remarkable. For example, in the region prior to breakup, for a 0·05 % Separan jet issuing from a 0·0216 cm nozzle at 460 cm/sec, the diameter of the threads connecting a series of droplets decreased from 0·01 cm to 0·004 cm over a length of 8 cm.

A Newtonian liquid of the same zero shear viscosity would break up in only 1–2 cm under these conditions.

The average diameter of the droplets formed after breakup as well as the size distribution were determined over a range of experimental variables for 0·05 % Separan jets and at a single flow condition for a 0·25 % Separan jet. The data taken with 0·05 % Separan show the droplet diameter to initially decrease

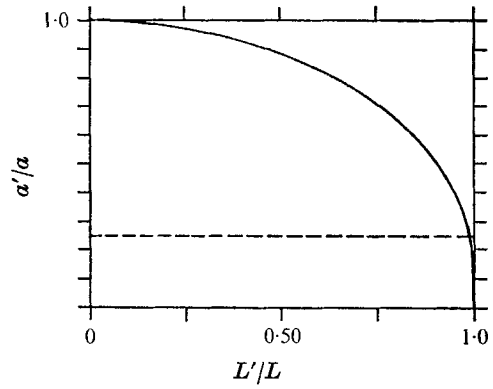

FIGURE 17. Non-dimensional plot of ratio of (a'/a) *vs.* (L'/L) for viscoelastic jets.

with jet velocity and then become independent of it. As shown in figure 18, the 0·05 % Separan droplets follow a normal distribution whereas the 0·25 % Separan droplets do not. From the photographs taken at the point of breakup it is seen that with 0·05 % Separan the connecting threads are absorbed into the main droplet. However, the threads in a 0·25 % Separan jet collapse and form small satellite droplets. Thus with the more concentrated viscoelastic fluid there would be a preponderance of small droplets included and the size distribution will assume the shape of a bimodal distribution (figure 18).

Duffie & Marshall (1953) investigated the droplet diameters and size distributions to be expected from the breakup of low speed, low viscosity Newtonian jets using capillary diameters and jet velocities similar to those employed in this study. Their data ware correlated by the empirical equation

$$D_g = 36(2a)^{0\cdot56}Re^{-0\cdot10}, \tag{33}$$

where D_g, the geometric mean diameter and a are in microns. For turbulent flow conditions, Miesse (1955) expressed the results of his Newtonian jet experiments in the form

$$D/2a = We^{-\frac{1}{3}}(23\cdot5 + 3\cdot95 \times 10^{-4}Re). \tag{34}$$

Based on the estimated zero shear viscosity of 0·25 % Separan, both (33) and (34) would predict a droplet diameter twice as small as that measured here. These discrepancies indicate that existing Newtonian correlations are inadequate to predict droplet data for viscoelastic jets such as 0·25 % Separan. The standard deviation and the coefficient of variation, C_v, obtained in this study of Separan

jet, however, were of the same order of magnitude as the results of Duffie & Marshall. The coefficient of variation, C_v, is defined as

$$C_v = \frac{[(\Sigma D_i^5/\Sigma D_i^3) - (\Sigma D_i^4/\Sigma D_i^3)^2]}{(\Sigma D_i^4/\Sigma D_i^3)^3},$$

where D_i is the diameter of droplet i.

4. Discussion of experimental results

In the theoretical analysis it has been shown that the growth rate of axisymmetric disturbances for any viscoelastic fluid is higher than that of a Newtonian fluid of the same zero shear viscosity, but smaller than that of an inviscid fluid. If the complex viscosity of the viscoelastic fluid could be readily measured,

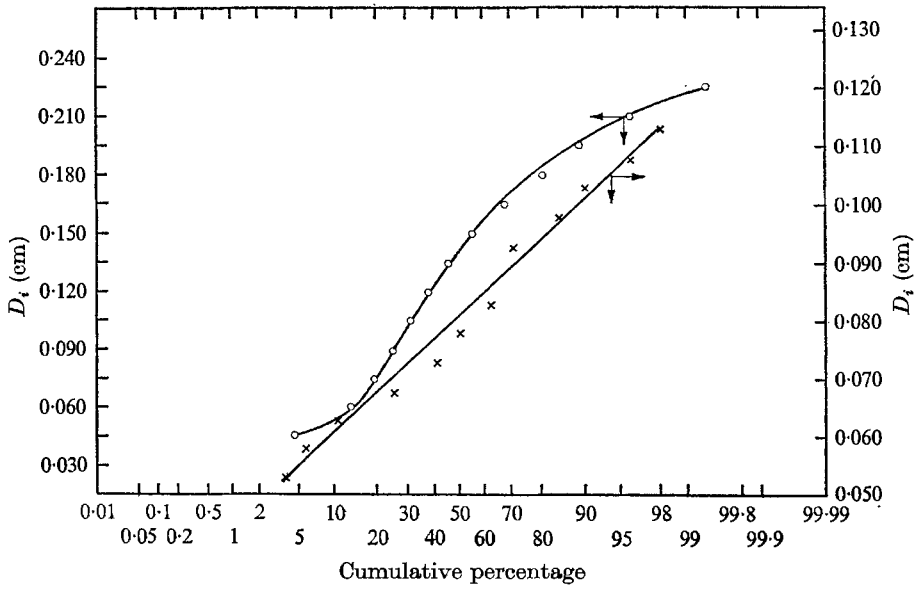

FIGURE 18. Droplet size distribution formed by breakup of 0·05 % Separan and 0·25 % Separan jets. ×, 0·05 % Separan; nozzle diameter, 0·0263 cm; jet velocity, 495 cm/sec; ○, 0·25 % Separan; nozzle diameter, 0·0216 cm; jet velocity, 1045 cm/sec.

then one could predict the growth rate as a function of wavelength, assuming that the liquid column is completely relaxed initially. However, for the dilute solutions used in these experiments, the complex viscosity cannot be determined and only a qualitative prediction can be made.

In the experiments, growth rates were not measured directly and comparisons of jet stability were made on the basis of the breakup length. This approach gives good agreement with Weber's theoretical predictions (equation (23)) for Newtonian liquids. The breakup lengths of 0·1 % Carbopol and 0·25 % SCMC were found to be shorter than those of a Newtonian fluid of the same zero shear viscosity, in agreement with theory. Actually, the breakup length of 0·1 %

Carbopol was even shorter than for an inviscid fluid and this phenomenon is not presently understood.

Contrary to what occurs in Newtonian liquids, the growth of the disturbance wave in 0·25 % SCMC does not lead to immediate breakup and the droplets remain connected for a considerable distance by thin threads. This thread formation seems to be typical of elastic liquids. No wave formation has been observed in highly elastic liquids such as 0·25 % Separan and 0·25 % Polyox. Even in relatively dilute solutions (0·05 % Separan) the waves which do appear initially are damped out. Instead, disturbances propagate as isolated droplets connected by random lengths of threads. In many cases, the threads are longer than any reasonable wavelength that could be associated with the droplet. These nonlinear disturbances occur at a distance which is shorter than the breakup length of a Newtonian liquid of comparable zero shear viscosity. Thus, one cannot conclude that the viscoelastic jet is more stable with respect to the growth of axisymmetric disturbance waves.

It has been observed for all the viscoelastic jets that the droplets which are formed are connected by threads which continually thin and lead to the eventual breakup of the jet. Two questions arise: why do the threads form, and what causes their remarkable stability? While the original jet does not show any increased stability as compared to a Newtonian jet, the connecting threads have a lifetime several fold higher than expected since viscoelastic jets, extruded from a nozzle which are of the same order of thickness as the threads, do not exhibit this increased stability.

Two reasons might explain this difference. First, a viscoelastic jet extruded from a nozzle which is of similar thickness as the thread has just experienced a high shear rate. The breakup time and relaxation time are of the same order of magnitude. Thus, the jet breaks up before the jet has relaxed and regained its shear dependent viscosity. However, the thin thread at a distance from the nozzle is derived from a much thicker jet which was less severely sheared in the capillary and which has also had time to partially relax. The second and more important difference is that the thread is under some stress as shown by the fact that it continues to thin. This stress might be caused by either the surface tension forces at the connexion to a droplet or by the relative motion of two droplets. Looking at photograph (*a*) of figure 9, plate 3, one might question this explanation as some threads look quite relaxed. However, the high speed movies indicate that a thread as seen in photographs (*a*)–(*j*) of figure 18 constantly changes its configuration and therefore must be undergoing some deformation.

The formation and stability of a thread might have a common explanation. During thread formation and during the thinning process, the liquid undergoes a flow which is characterized as an extrusion or stretching flow. Coleman & Noll (1962), Lodge (1964, pp. 114–18) and White (1964) have shown that the behaviour of elastic liquids under tension is completely different from that in shear flow in the sense that viscoelastic liquids may exhibit a sharp increase in elongational viscosity when subjected to stretching flows. This phenomenon has also been used to explain the fact that one can spin an elastic liquid of low viscosity whereas Newtonian liquids are spinnable only at high viscosities. Nitschmann & Schrade

(1948), Lodge (1960), Ziabicki & Krystyna (1960), Ballman (1965) and Marshall & Metzner (1967) have related the increased spinnability of elastic liquids to the viscosity increase in a stretching flow. Regretfully, a rigorous quantitative treatment of spinning is not available and the above arguments are somewhat speculative.

5. Concluding remarks

A linearized stability analysis has shown that a liquid jet of a viscoelastic fluid exhibits a more rapid growth of axisymmetric wave disturbances than a Newtonian fluid of the same shear viscosity and that this result is independent of the form of the constitutive equation chosen. Experiments in weakly elastic fluids have confirmed this expectation, whereas data on fluids with more pronounced elastic properties indicate that non-linear phenomena are dominating.

Considerably more work is necessary before the complex behaviour of elastic fluids will be fully understood and it is hoped that the present paper has at least pointed out some of these problems. Finally, it should be clear that for all practical purposes the atomization behaviour of elastic liquids must be considered together with their flow behaviour. Thus, a Napalm jet used as a flame thrower has a zero shear viscosity so high that a comparable Newtonian liquid could not be extruded through a nozzle. If this were possible, the Newtonian fluid would probably be stable for all practical purposes. However, as the strongly differing results of 0·1 % Carbopol and 0·25 % Separan show, the stability of such shear thinning liquid jets cannot be predicted solely from a knowledge of their shear dependent viscosity, as their elastic properties are also important.

In some cases we are interested in jellifying a liquid or increasing its zero shear viscosity and still be able to atomize it. The results with 0·1 % Carbopol indicate that this could be achieved by choosing the correct thickening agent.

This research has been supported by NASA Grant NGR-33-013-009. Parts of this paper have been taken from the doctoral theses of Mr M. Goldin and Mr J. Yerushalmi. The authors also would like to thank Prof. S. Katz (City College) for his many helpful discussions and Prof. A. B. Metzner (University of Delaware) and Prof. W. H. Schwarz (University of Stanford) for contributing their data on Separan solutions.

REFERENCES

Ballman, R. L. 1965 *Rheol. Acta*, **4**, 137.
Biot, M. A. 1954 *J. Appl. Phys.* **25**, 1385.
Bland, D. R. 1960 *The Theory of Linear Viscoelasticity*. Oxford: Pergamon.
Coleman, N. D. & Noll, W. 1962 *Phys. Fluids*, **5**, 840.
Dodge, D. W. & Metzner, A. B. 1959 *A.I.Ch.E. J.* **5**, 189.
Duffie, J. A. & Marshall, W. R. 1953 *Chem. Engng Prog.* **49**, 417, 480.
Grant, R. P. & Middleman, S. 1966 *A.I.Ch.E. J.* **12**, 669.
Huppler, J. D. 1965 Ph.D. thesis. University of Wisconsin.
Hurd, R. E. 1962 B.Ch.E. Thesis. University of Delaware.
Kapoor, N. N. 1963 M.S. thesis. University of Minnesota.

LODGE, A. S. 1960 *Collogue Intnl. de Rhel.* Paris, France.
LODGE, A. S. 1964 *Elastic Liquids.* London: Academic.
MARSHALL, R. J. & METZNER, A. B. 1967 *Ind. Engng Chem. Fundamentals*, **6**, 393.
MERRILL, E. W. 1959 *Ind. Engng Chem.* **51**, 868,
MIDDLEMAN, S. 1965 *Chem. Engng Sci.* **20**, 1037.
MIESSE, C. C. 1955 *Ind. Engng Chem.* **37**, 1690.
NITSCHMANN, H. & SCHRADE, J. 1948 *Helv. Chim. Acta*, **31**, 297.
OLIVER, D. R. 1966 *Canad. J. Chem. Engng* **44**, 100.
RAYLEIGH, LORD 1879 *Proc. Roy. Soc.* A **29**, 71.
RAYLEIGH, LORD 1882 *Phil. Mag.* **34**, 145.
SEYER, F. A. & METZNER, A. B. 1967 *Canad. J. Chem. Engng* **45**, 121.
SCHWARZ, W. H. 1968 Submitted for publication, University of Stanford.
SHERTZER, C. R. 1965 Ph.D. thesis. University of Delaware.
TOMOTIKA, S. 1935 *Proc. Roy. Soc.* A **150**, 322.
TURIAN, R. M. 1964 Ph.D. thesis. University of Wisconsin.
WEBER, C. 1931 *Z. angew Math. Mech.* **11**, 136.
WELLS, C. S. 1965 *AIAA J.* **3**, 1800.
WHITE, J. L. 1964 *J. Appl. Poly. Sci.* **8**, 2339.
ZIABICKI, A. & KRYSTYNA, K. 1960 *Kolloid Z.* **171**, 111.